https://doi.org/10.5194/essd-2022-91
Preprint. Discussion started: 16 March 2022

Open Access Earth System Science Data Discussions

A database of radiogenic Sr-Nd isotopes at the "three poles"

Zhiheng Du[a], Jiao Yang[a], Lei Wang[b], Ninglian Wang[c], Anders Svensson[d], Zhen Zhang[e], Xiangyu Ma[f], Yaping Liu[a], Shimeng Wang[a], Jianzhong Xu[a], Cunde Xiao[b*]

[a]State Key Laboratory of Cryospheric Science, Northwest Institute of Eco-Environment and Resources, Chinese Academy of Sciences, Lanzhou 730000, China

[b]State Key Laboratory of Land Surface Processes and Resource Ecology, Beijing Normal University, Beijing 100875, China

[c]College of Urban and Environmental Sciences, Northwest University, Xi'an 710127, China

[d]Centre for Ice and Climate, Niels Bohr Institute, University of Copenhagen, Copenhagen, Denmark

[e]School of Spatial Informatics and Geomatics Engineering, Anhui University of Science and Technology, Huainan 232001, China

[f]Qingdao Blue Thinking Information Technology Co.Ltd, Qinggao 266555, China

*Correspondence and requests for materials should be addressed to CD. X (cdxiao@bnu.edu.cn).

Abstract: The radiogenic isotope compositions of strontium (Sr) and neodymium (Nd) on the surface of the Earth are powerful tools for tracing dust sources and sinks on Earth's surface. To differentiate between the spatial variabilities of aeolian dust sources in key cryospheric regions at the three poles (including the 'Third Pole' covering the high mountainous area in Asia, the Arctic and Antarctica), a dataset of the Sr-Nd isotopic compositions from the terrestrial extremely cold or arid environments in this study was compiled, similar to the method of Blanchet (2019). The database identified snow, ice, sand, soil (loess) and sediment from the modern dust samples and paleoclimatic records of the three poles based on 43 different references, with a total of 967 data points. There are 274 data points from the third pole, 302 data points from the Arctic, and 391 data points from Antarctica. The sampling and measurement methods and the quality of these data are recognized and introduced. For each pole, geographical coordinates and other information are provided. The main scientific purpose of this dataset is to provide our own measurements and collect documentation for the Sr-Nd dataset, which will be useful for determining the sources and transport pathways of dust at the three poles and to investigate whether multiple dust sources are present at each of the poles. This dataset provides exhaustive detailed documentation of the isotopic signatures at the three poles during specific time intervals, which are useful for understanding the dust sources or sinks of the three poles. The datasets are available from the National Tibetan Plateau Data Center (https://doi.org/10.11888/Cryos.tpdc.272100, Du et al., 2022).

Keywords: Radiogenic isotopic dataset, third pole, Arctic Ocean, Greenland and Antarctica ice sheets, Dust provenances.

1. Introduction

The role of mineral dust in the Earth system extends well beyond its impact on the energy balance and involves the interactions with the carbon cycle, the cryosphere, and public health on global scales (Shao et al., 2011). The transport of dust from the low mid-latitudes, which contain major deserts that are dust sources, to the Arctic region or Antarctic ice sheet is sensitive to amplified high-latitude climatic variability (Lambert et al., 2013: Struve et al., 2020). The isotopic compositions of the radiogenic isotopes of strontium (Sr) and neodymium (Nd) are a powerful tool for tracing dust sources and sinks because their characteristics are significantly different

https://doi.org/10.5194/essd-2022-91
Preprint. Discussion started: 16 March 2022

on the surface of the Earth (including sand, sediment, loess, aeolian deposits and snow) (Grousset et al., 2005). Therefore, the combination of different isotopic signatures, specifically $^{87}Sr/^{86}Sr$ and $^{143}Nd/^{144}Nd$, has proven be useful in discriminating different dust source areas in the earth science (Biscaye et al., 1997).

Aeolian dust from East Asian deserts is transported globally and has been found in Greenland snow and ice based on Sr-Nd data in modern environments (Bory et al., 2003a; Bory et al., 2003b; Lupker et al., 2010). Sr-Nd data in the Greenland ice sheet (GrIS) deep ice core also emphasize the contribution of aeolian dust from Asian deserts (Biscaye et al., 1997; Svensson et al., 2000). The Sahara was taken as an additional dust source for the GrIS based on NEEM and Dye-3 ice cores (Han et al., 2018; Lupker et al., 2010). This situation has been attributed to the lack of detailed observational data in the remote Arctic; therefore, the prediction ability of the impact of changing aeolian dust loading on cryospheric science has been limited in the Northern Hemisphere (NH). Therefore, aeolian dust from various source regions, including the Saharan Desert in North Africa or the Gobi and Taklamakan Deserts in Asia, is transported to the GrIS, there are still great uncertainties. As much more Sr-Nd data were measured, and it is necessary to reassess these data on the dust sources for the Arctic.

The transport of aeolian dust from natural desert regions has also been found in modern snow and ice records at the third pole (Wu et al., 2010; Xu et al., 2012; Du et al., 2015; Dong et al., 2018). Many studies have focused on dust transport from the western Chinese deserts to the Chinese loess plateau (CLP), Pacific Ocean and even the GrIS (Chen et al., 2007; Du et al., 2015; Wu et al., 2010; Wei et al., 2021). However, it is still a controversial issue; for example, recent results have emphasized that aeolian dust from local sources contributes significantly to high mountain glaciers

https://doi.org/10.5194/essd-2022-91
Preprint. Discussion started: 16 March 2022

(Du et al., 2019a; Wei et al., 2021). On longer time scales, Sr isotope geochemistry in fluvial sequences (12.7-4.8 Ma) reveals aeolian dust input and the southeastward expansion of the dust impact on river water occurred on the northeastern TP (Ruan et al., 2019). Therefore, the amounts of Sr-Nd data measured in snow, soil, sediment, sand and other samples should be integrated into a dataset to better serve the environmental and climatic sciences studying the third pole in the future.

The Sr and Nd isotope data from insoluble dust in snow samples along the Zhongshan-Dome A transect, East Antarctica, indicate that long-distance natural dust primarily originates from Australia and that local dust originates from ice-free areas (Du et al., 2018). The Sr-Nd characteristics of snow layers at the Berkner Island ice sheet in western Antarctica, for most of the year, are data support scenarios that involve contributions from proximal sources (Bory et al., 2010). Sr-Nd in the Taylor Glacier zero-age ice samples and snow samples from Roosevelt Island could be a mixture of at least two local sources (Winton et al., 2016a; Aarons et al., 2017). The Sr and Nd data from East Antarctica ice cores during the Holocene indicate a well-mixed atmospheric background involving a mixture of two or more sources in the SH (Aarons et al., 2016, 2017; Delmonte et al., 2019). Southern South American (SSA) dust is considered to have been the dominant type of dust during glacial periods in the Southern Hemisphere (SH) (Grousset et al., 1992). The amount of isotopic information is currently adequate for Patagonian and non-Patagonian mineral aerosols exported from southern South America (Gaiero et al., 2007; Delmonte et al., 2010a, b, 2019; Aarons et al., 2017). However, because some ice-free areas are located at the present-day margin of the East Antarctic ice sheet (EAIS), data are insufficiently documented, and much is still known about the cycle in the SH. Major efforts have attempted to solve the 'puzzle' of the origin of the potential source areas that contribute dust to the Southern Ocean and the whole Antarctic ice sheet (Gili et al., 2021). The Sr-Nd data in the entre Antarctica ice sheet have an uneven distribution. Measuring Sr-Nd stable isotopic compositions in ice cores from Antarctica is a major challenge. Therefore, these data characteristics and measurement methods are discussed in detail.

The answers to these questions have been hindered by a paucity of Sr-Nd data, which provide information on the local and potential dust sources. For these reasons, we measured Sr-Nd data in some samples and collected Sr-Nd data in the literature at the three poles (Fig. 1, Table 1). Therefore, the objective of this work was to produce a compilation of published and unpublished data from the three poles, further discuss the aeolian dust contributions from high-elevation regions, and trace the potential aeolian dust transport paths in Greenland and Antarctic ice sheets. Similar to the method of Blanchet (2019), here, we compile published and unpublished Sr-Nd data with an integrated filtering system from three remote poles, in which these data were collected in terrestrial extremely cold or arid environments with data augmentation, and most of the data were not included in the previous dataset. The measurements of Sr and Nd isotopic ratios used thermal ionization mass spectrometry for most samples. The dataset will help trace modern natural dust, reconstruct past environments, and extend the database of terrestrial radiogenic Sr and Nd isotopes in the Earth and environmental sciences.

2. Sample collecting, data measuring and processing

Sr-Nd data in surface sand, soil or loess samples were collected from own research and literature from three poles (including Chinese deserts and the Tibetan Plateau (TP), the Greenland and Antarctic ice sheets, the Arctic, Australia, southern South America (SSA), Southern Africa (SA) and New Zealand) (Fig. 1). The sand

https://doi.org/10.5194/essd-2022-91
Preprint. Discussion started: 16 March 2022

(soil and loess) samples were collected from Chinese deserts and the TP, including the Taklimakan Desert in the Tarim Basin, the Gurbantunggut Desert in the Junggar Basin, the Qaidam Desert in the Qaidam Basin, and the Badain Jaran and Tengger Deserts, as well as the TP and Chinese loess Plateau (CLP) (Fig. 2, Table 2). Sand or soil samples in the Arctic were also collected from Ny-Ålesund on the western coast of Svalbard; Barrow, Alaska; and Kangerlussuaq, West Greenland (Table 3). Cryoconite samples were collected from the surface at different elevations in glaciers from western China and GrIS (Table 3). The sand (soil, loess and other types) samples were sampled in Australia, southern South America, Southern Africa and New Zealand, and information can be found in Table 4. Four sand samples collected on King George Island and eleven sand samples collected on Inexpressible Island in the Ross Sea, West Antarctica, were measured in this study (Table 4). In general, the upper 2 or 5 cm of surface topsoil (sand) was collected with a trowel and stored in precleaned plastic bags or bottles. Surface sediments from shelves and ridges in the Arctic Ocean (Table 3), which were mostly retrieved from core archives, were subsampled in the upper 10 cm of the core tops (with rare exceptions) (Maccali et al., 2018). Different grain sizes (<5 μm, <10 μm, <71 μm, <75 μm and <100 μm fractions and bulk) of surface soil or sand were extracted by the sieving method (Chen et al., 2007; Maccali et al., 2018; Du et al., 2018, 2019a, b; Wei et al., 2021).

The snow samples were collected in the most favourable sector to avoid possible pollution by camp activities (upwind from the camp according to prevailing summer wind directions). Snow samples were collected from the snowpit at a vertical resolution of 5–20 cm, following the clean-hands protocol with sampling personnel wearing integral Tyvek® bodysuits, nonpowdered gloves and masks to avoid possible contamination (Xu et al., 2012). In this study, one 1.0 m snowpit with a resolution of

https://doi.org/10.5194/essd-2022-91
Preprint. Discussion started: 16 March 2022

10 cm was dug in the East Greenland ice sheet (GrIS), and four fresh snow samples (M1, M2, M3 and M4) were sampled on sea ice in the Arctic Ocean during MOSAIC (Multidisciplinary drifting Observatory for the Study of Arctic Climate) in October 2020 in this study. Surface fresh snow (2-10 cm) samples at different resolutions (with different thicknesses, widths and lengths) in Greenland and Antarctica ice sheets were excavated and placed in 5 L Whirl-Pak bags (Du et al., 2018; Du et al., 2019a, b). Three horizontal snow layers were collected for Greenland and Antarctica snowpits (Bory et al., 2003b; Bory et al., 2010). The dust from snow samples was extracted using three methods. First, melt water was immediately filtered through a membrane filter (with 0.2 or 0.45 μm pore sizes) by using precleaned (acid washed) plastic filtration units (Wu et al., 2010). Second, melt water was centrifuged, with the unit of at revolutions per minute (rpm), the supernatant was discarded and the remaining water was vacuumed freeze-dried (or evaporated). The filtration was completed in a class 1000 clean room (Xu et al., 2009). Third, the melt water was evaporated for obtaining sufficient dust. The ice cores were kept frozen and sampled at different intervals, which were drilled from the TP, Greenland and Antarctica ice sheets. Detail of geographical coordinates and original information can be found in Tables 1-4 and references. The dust in the ice core wass extracted using the same method as that for the snow samples. Snow or ice core samples are nearly bulk samples or had different grain sizes (>0.2 μm, > 0.45 μm, > 0.45 μm and <30 μm) (Du et al., 2015, 2019b; Bory et al., 2003 a,b; Bory et al., 2010; Lupker et al., 2010; Wu et al., 2010). In particular, the soluble fraction of some ice core samples was measured, which can indicate marine or anthropogenic pollutant signals (Lupker et al., 2010; Du et al., 2015).

Sr-Nd isotope datasets from snow, ice core, sand, sediment, soil and loess

https://doi.org/10.5194/essd-2022-91
Preprint. Discussion started: 16 March 2022

samples from the third pole, Arctic and Antarctica were compiled. In total, 274 (snow, ice, soil and sand (loess) samples) data points were collected from the third pole, 302 data points (snow, ice, cryoconite, sand, soil and sediment) were collected from the Arctic (Table 3), and 391 data points (snow, ice, soil and sediment) were collected from the SH and Antarctic ice sheet. The locations of these samples are shown on maps provided below. To keep the naming scheme uniform, the dataset assembled the names of each sample based on the work by Blanchet (2019). This dataset adds the Sr-Nd isotope data from extreme cold and drought environments at the three poles and built by incorporating data from the literature and our own database; in particular, units and geographical coordinates are marked in the dataset. An overview of the input data is shown in Table 1. The study focuses on the large amounts of different data, including data on snow, ice, sand, soil, loess, sediment, etc. The data are based on our own measurements, author contributions (data published and provided by first author) and literature searches. Data were collected from 43 different references with 967 data points in total.

All subsequent procedures were performed in clean lab facilities. The sand, loess, sediment, cryoconite and dust extracted from snow or ice cores were generally digested with ultrapure acid (HNO_3, HF and $HClO_4$ or HNO_3, HF and HCl), and $^{87}Sr/^{86}Sr$ and $^{144}Nd/^{146}Nd$ ratios were determined by the different types of thermoionization mass spectrometry (TIMS). Sr-Nd values, with uncertainties are expressed as $\pm 2\sigma \times 10^{-6}$ (2 standard errors of the mean) and also can be found in the original references. The $^{144}Nd/^{146}Nd$ isotopic composition is expressed as:

$\varepsilon_{Nd}(0) = ((^{143}Nd/^{144}Nd)_{Sample}/(^{143}Nd/^{144}Nd)_{CHUR} - 1) \times 10^4$, where $(^{143}Nd/^{144}Nd)_{CHUR} = 0.512638$, where CHUR stands for chondritic uniform reservoir and represents a present-day average Earth value $(^{143}Nd/^{144}Nd)_{CHUR} = 0.512638$ (Jacobsen &

https://doi.org/10.5194/essd-2022-91
Preprint. Discussion started: 16 March 2022

Wasserburg 1980; Blanchet, 2019).

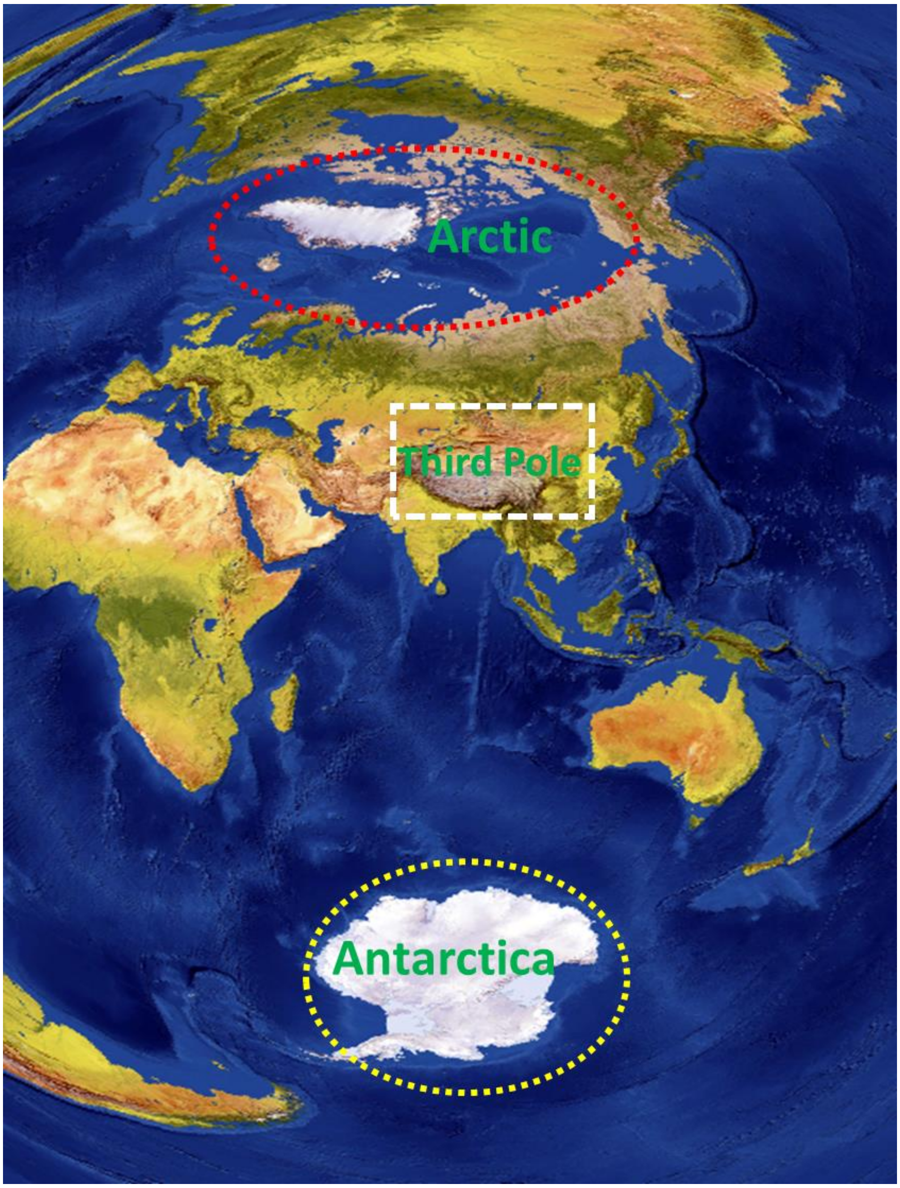

Fig. 1. Map of the sampling regions in the three poles (the third pole, Arctic and Antarctica are indicated with different coloured circles) in this study (The background of this figure is from ArcGIS).

3. Data descriptions

https://doi.org/10.5194/essd-2022-91
Preprint. Discussion started: 16 March 2022

3.1. The Sr-Nd data measurement of glaciers at the third pole

Table 2 provides an overview of the information (the number of glaciers; subregions; glacier name; site name: name of the sampling site where the samples were taken; longitude and latitude; sample type and elevation) from the third pole, which are used to fingerprint potential source areas (PSAs) based on the isotopic signatures of these snow and sand (soil) samples (Fig. 2; Table 2). The grain size effect in different samples is presented in the dataset for better illustration using these data. The grain size effect in different samples resulted in $^{87}Sr/^{86}Sr$ ratio variations (Chen et al., 2007; Svensson et al., 2000; Gili et al., 2021). The different acid leaching methods also have a weak effect on Sr isotopic composition in the silt and clay fractions (Schettler et al., 2009; Naoko et al., 2010; Meyer et al., 2011). Therefore, this work attempts to build a new database that includes the different gran sizes and acid leaching methods.

This feature validates the use of the geological characteristics from Sr-Nd isotopic data; as an example, we can use the sorting criteria for determining PSAs based on these data. For introducing these data based on geographic features, six isotopic subregions across the entire third pole were divided as follows (Fig. 3):

Region I: Samples from glaciers located in the Altai Mountains include the snow samples from Musidao glacier and Altay, and sand samples from the Gurbantunggut Desert, with $\varepsilon_{Nd}(0)$ values from -6.55 to -1.2 and $^{87}Sr/^{86}Sr$ values ranging from 0.705483 to 0.71480. The highest $\varepsilon_{Nd}(0)$ values were observed in this region (Chen et al., 2007; Xu et al., 2012; Du et al., 2019a).

Region II: Samples from the glaciers on the northern margin of the TP include snow samples from the Tienshan Mountains (Tienshan No. 1 glacier and Miaoergou ice cap) and Kunlun Mountains (Muztagata), as well as sand samples from the

https://doi.org/10.5194/essd-2022-91
Preprint. Discussion started: 16 March 2022

Taklimakan Desert, with $\varepsilon_{Nd}(0)$ values from -11.8 to -6.9 and $^{87}Sr/^{86}Sr$ values from 0.70842 to 0.728641 (Chen et al., 2007; Nagatsuka et al., 2010; Du et al., 2015; Xu et al., 2012; Wei et al., 2019).

Region III: The Sr-Nd isotopic characteristics of the glaciers and sand/soil in the interior of the TP include $\varepsilon_{Nd}(0)$ values ranging from -10.5 to -8.6 and $^{87}Sr/^{86}Sr$ values from 0.713192 to 0.721786 (Xu et al., 2012; Du et al., 2019a; Wei et al., 2021).

Region IV: The Sr-Nd isotope data from snow and sand (soil) samples from glaciers in the Himalayan Mountains (East Rongbuk, Jiemayangzong and Yala) include $\varepsilon_{Nd}(0)$ values ranging from -28.1 to -10.5 and $^{87}Sr/^{86}Sr$ values ranging from 0.724542 to 0.757407 (Xu et al., 2012; Wei et al., 2021).

Region V: Samples from the glaciers in the Qilian Mountains include snow samples from the Qilian Mountains and sand (soil and loess) samples from the Hexi Corridor, with $\varepsilon_{Nd}(0)$ values from 0.712349 to 0.73211 and $^{87}Sr/^{86}Sr$ values from -15.7 to -7.0 (Wei et al., 2017; Dong et al., 2018). The $\varepsilon_{Nd}(0)$ values have an increasing trend along the Hexi Corridor from west to east: -15.7–-12.9 for Laohugou No. 12 glacier (local soil: -13.6), -13.7–-8.58 for Qiyi, -13.8–-13.6 for Shiyi glacier (local soil: -13.8–-13.6), -12.1–-12.0 for Dabanshan snowpack, and -10.9–-7.0 for Lenglongling glacier (Fig. 2, Dong et al., 2018). It is very clear that, based on local soil data, regional dust makes a significant contribution to these glaciers.

Region VI: Samples from the glaciers in the eastern TP include snow and soil samples from the Hengduan Mountains, with $\varepsilon_{Nd}(0)$ values from -17.1 to -10.1 and $^{87}Sr/^{86}Sr$ values from 0.717145 to 0.735863 (Xu et al., 2012; Dong et al., 2018).

There is an increasing $^{87}Sr/^{86}Sr$ trend from north (region I) to south (region V), and there is a decreasing $\varepsilon_{Nd}(0)$ trend from north (region I) to south (region V). The maximum $^{87}Sr/^{86}Sr$ ratios and minimum $\varepsilon_{Nd}(0)$ values were observed in region V (Fig.

https://doi.org/10.5194/essd-2022-91
Preprint. Discussion started: 16 March 2022

3). The Sr-Nd data in the third pole have relatively narrow ranges with distinct features, while the largest uncertainty was observed from Region IV. The same measurement methods were used in these references (Du et al., 2015, 2019a; Dong et al., 2018, Wei et al., 2019, 2021), and a similar measurement method was used by Xu et al. (2012). Different methods were used by the other two references (Chen et al., 2007; Nagatsuka et al., 2010). However, the data results seem to remain fully consistent with these references.

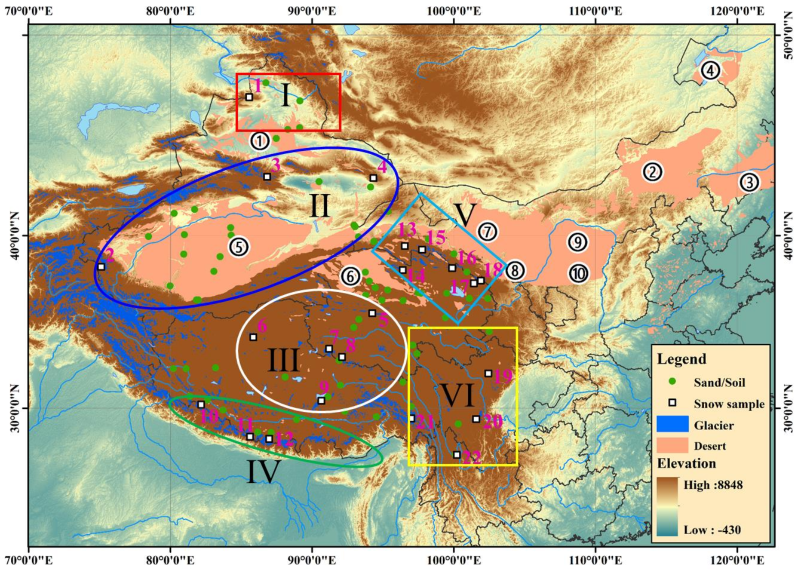

Fig. 2. The glacier and desert distributions in western China (the different coloured oval and rectangular shapes represent six sub-regions based on Sr-Nd data; pink numbers and white rectangles represent 22 glaciers, for which the names of glaciers are shown in Table 2, and green solid circles represent sand/soil samples; the numbered circles represent the ten deserts of China) (This figure was created with ArcGIS).

https://doi.org/10.5194/essd-2022-91
Preprint. Discussion started: 16 March 2022

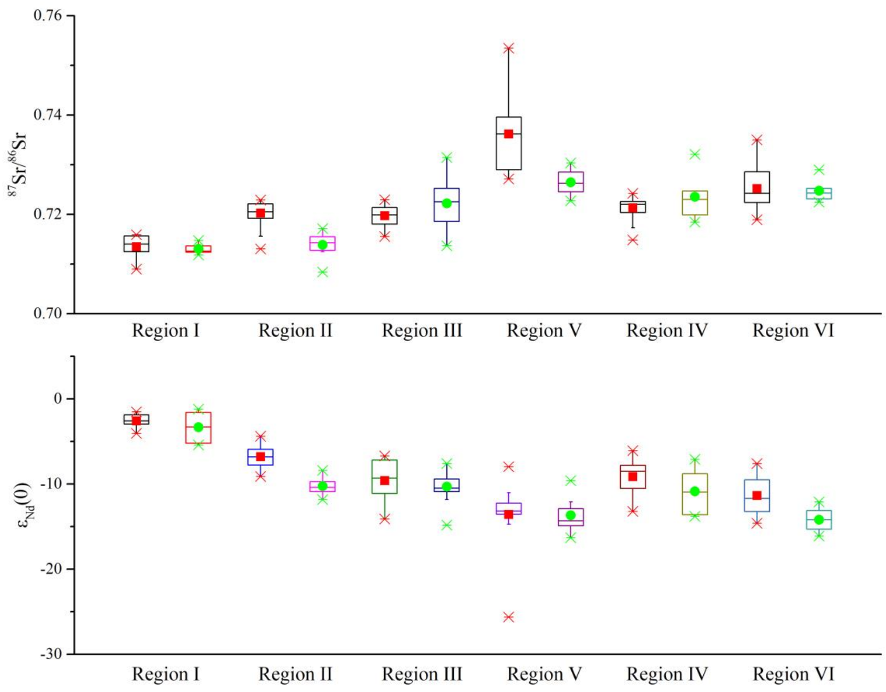

Fig. 3. Box plot for the Sr-Nd isotopic signatures of third pole PSAs and snow samples. Samples are located in each PSA region based on the data from Table 2. The mean Sr-Nd values are shown as red rectangles for sand or soil samples and green solid cycles for snow samples.

3.2. Sr-Nd data in natural dust or sediment from the Arctic

Considerable Sr-Nd isotope data have been obtained from modern snow/ice samples from the Arctic and surface and sea ice-transported sediments from the Arctic Ocean, which covers the entire Arctic. Sand samples from PSAs (East Asian and Saharan deserts) are also collected. Therefore, these data are useful for tracing the terrigenous material transport for the Arctic. For user-friendly selection of the Sr-Nd data according to the modern environment characteristics and the geographical location, the 11 subregions were presented in the entire Arctic as follows (Fig. 4). The patterns of the geographical zone have been similarly defined regarding seas and

https://doi.org/10.5194/essd-2022-91
Preprint. Discussion started: 16 March 2022

drainage basins of the main river systems, as divided by Maccali et al. (2018).

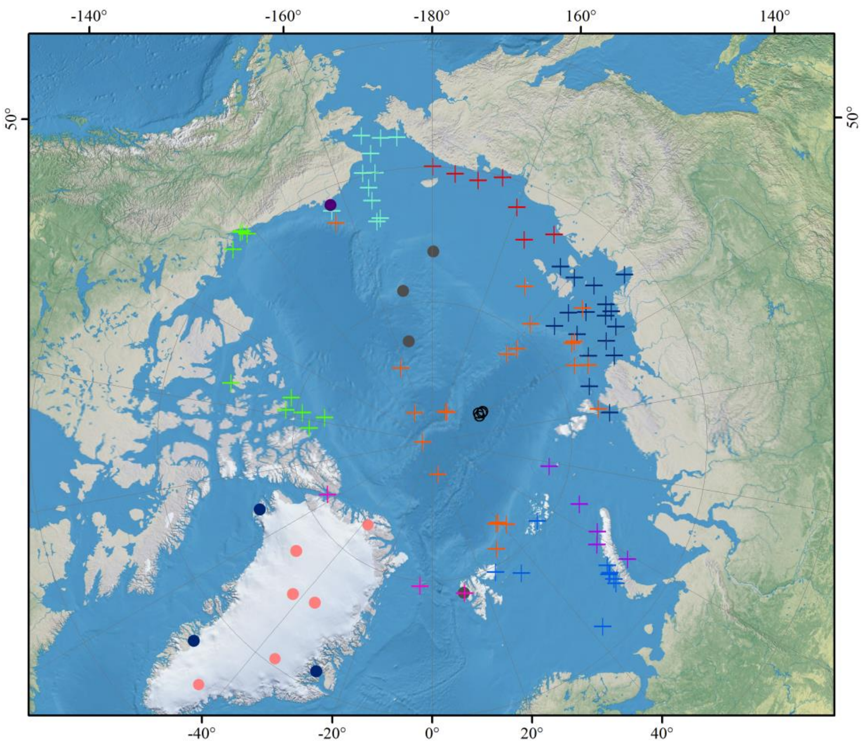

Fig. 4. Sampling distribution sites in the Arctic. The snow and cryoconite (sand or soil) sampling sites are denoted with circles, and sediment samples are marked with crosses (Table 3). 1. GrISS (Greenland ice sheet snow samples with orange solid cycles); 2. GrIS-SSS (Greenland ice sheet sand or sediment samples with black solid cycles); 3. SV (Svalbard sand or soil samples with magenta crosses); 4. AOS (Arctic Ocean snow samples with grey solid and black cycles); 5. AOSS (Arctic Ocean sea ice sediment samples with orange crosses); 6. BS (Barents Sea sediment samples with blue crosses); 7. KS (Kara Sea sediment samples with violet crosses); 8. LS (Laptev Sea sediment samples with black crosses); 9. ESS (East Siberian Sea sediment samples with red crosses); 10. BCS (Bering-Chukchi Sea sediment samples with cyan

https://doi.org/10.5194/essd-2022-91
Preprint. Discussion started: 16 March 2022

crosses); 11. MCAA (Mackenzie-Canadian Arctic Archipelago sediment samples with green crosses) (This figure was created with ArcGIS).

3.2.1 Sr-Nd data from snow/ice and sand samples of the Greenland ice sheet

Sr-Nd data from different types of samples (snow/ice and sand samples) of samples were collected from the GrIS. The snow samples were measured in the bulk or >0.2 μm (0.45 μm) fraction, but it is noted that some shallow ice core samples from the GrIS were filtered through two precleaned 0.2 μm and 30 μm filters (Lupker et al., 2010). For some ice core samples, dust was subsequently extracted by evaporation (Bory et al., 2003a). Sand samples were sieved to <71 μm in this study, and soil, cryoconite, moraine, and englacial dust samples were used in bulk (Nagatsuka et al., 2016). Sr-Nd data from the East Greenland Ice Core Project (EGRIP) and the North GRIP (NGRIP) were measured via snowpits. Ice core samples were collected from GRIP, GISP2, NEEM and RECAP. Sr-Nd data exhibit large differences between snow and ice core samples (Fig. 5, Tables 1 and 3). In addition, the shallow ice core samples were collected from Renland, Site A, Hans Tausen and Dye 3 (Du et al., 2019b; Bory et al., 2003a). Cryoconite, moraine, and englacial dust samples were collected from Kangerlussuaq, Thule, Scoresby Sund and Kong Christian X Land of the GrIS (Nagatsuka et al., 2016; Simonsen et al., 2019).

The Sr-Nd data indicated that the dust sources were variable and showed complicated dust sources in the same location for NGRIP snow (Bory et al., 2002; Bory et al., 2003b). As much more Sr-Nd data from the sand, soil, cryoconite, moraine, and englacial dust samples in the peripheral of the GrIS were measured, $^{87}Sr/^{86}Sr$ values are the highest and the $^{143}Nd/^{144}Nd$ ratios are the least radiogenic in these samples (Table 3). Compared with Sr-Nd data in NGRIP and EGRIP snowpits, much larger variations were observed for $\varepsilon_{Nd}(0)$ in the EGRIP snowpit, and relatively

Open Access Earth System Science Data Discussions

larger $^{87}Sr/^{86}Sr$ values were observed in the NGRIP snowpit (Bory et al., 2002; Bory et al., 2003b). Although the Sr-Nd isotopic ratios indicated Asian deserts might be the main dust source for the GrIS. The ice-free region around the GrIS might be another source for the interior GrIS. The Sr and Nd isotopic data in sediment samples collected from the Scoresby Sund region by Simonsen et al. (2019) are as follows: the $^{87}Sr/^{86}Sr$ ratios range from 0.709689 to 0.736137, and the $\varepsilon_{Nd}(0)$ values range from -15.7 to -10.1. Combining Sr-Nd values in snow (Renland, Site A, Hans Tausen and Dye 3) and Dye 3 shallow ice core samples, the results showed that local dust sources may contribute some of the dust to the inland regions and that the Sahara is also the most likely additional source (Lupker et al., 2010). Therefore, the local dust for the free ice of the GrIS is another dust source, which may have been neglected in previous studies.

To compare the data during the same period, therefore, Sr-Nd data from the deep ice core were not included in Fig. 6. The mainstream view of the provenance of dust in inland Greenland deep ice cores (GISP2 and GRIP) is that the dust is from the eastern Asian deserts (the Gobi and Taklamakan Deserts) based on the best geochemical matches during the last glacial period (Biscaye et al., 1997; Svensson et al., 2000; Újvári et al., 2015). High-resolution Sr isotope data from the Greenland NEEM ice core suggested that there was a significant Saharan dust influence in Greenland during the last glacial period (Han et al., 2018). The Sr-Nd data (>5 μm) in Holocene RECAP ice core samples are attributed to proximal dust sources; however, the resolution of the data is approximately one thousand years (Simonsen et al., 2019). In addition, the Sr-Nd data in Greenland deep ice core samples, which have low resolutions and represent multiyear averages with no seasonal or interannual variations (60 to 200 cm or 30-150 years), need to be considered (Biscaye et al., 1997;

https://doi.org/10.5194/essd-2022-91
Preprint. Discussion started: 16 March 2022

Open Access Earth System Science Data Discussions

Svensson et al., 2000).

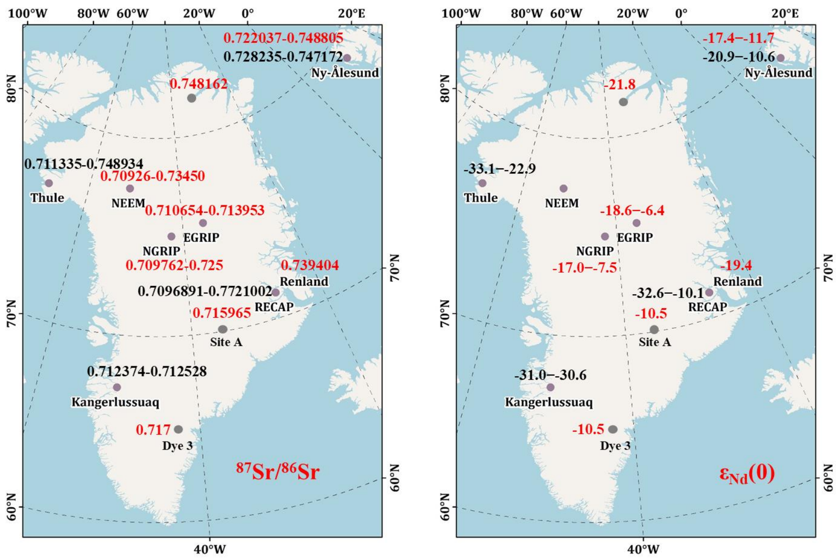

Fig. 5. $^{87}Sr/^{86}Sr$ and $\varepsilon_{Nd}(0)$ values of insoluble dust in snow or ice core (red) and sand/soil (black) samples from the Ny-Ålesund, Svalbard and GrIS (Bory et al., 2002; 2003a; Svensson et al., 2000; Biscaye et al., 1997; Lupker et al., 2010; Nagatsuka et al., 2016; Han et al., 2018; Du et al., 2019b) (This figure was created with ArcGIS).

3.2.2 Sr-Nd data from snow and sediment samples in the Arctic Ocean

The $^{87}Sr/^{86}Sr$ values are higher and $\varepsilon_{Nd}(0)$ values are lower in snow and sand samples from Ny-Ålesund, Svalbard (SV), snow samples were measured in bulk and sand samples were measured in the <71 μm fraction (Fig. 6, Du et al., 2019b). The Sr-Nd data in snow samples from sea ice were measured in bulk, and four of these samples were collected from near the North Pole in the western Arctic Ocean by MOSAIC (October 2020) in this study (Figs. 4 and 6). However, the new $\varepsilon_{Nd}(0)$ data have much more negative $\varepsilon_{Nd}(0)$ values (-20.8 to -19.6), which are very different from previous results and cannot be explained by low latitude potential dust sources (Du et

https://doi.org/10.5194/essd-2022-91
Preprint. Discussion started: 16 March 2022

al., 2019b). As shown in Fig. 6, the lowest ε_{Nd} values were observed along the ice-free periphery of the GrIS and SV; therefore, these ice-free regions are potential dust sources for natural dust in the Arctic Ocean.

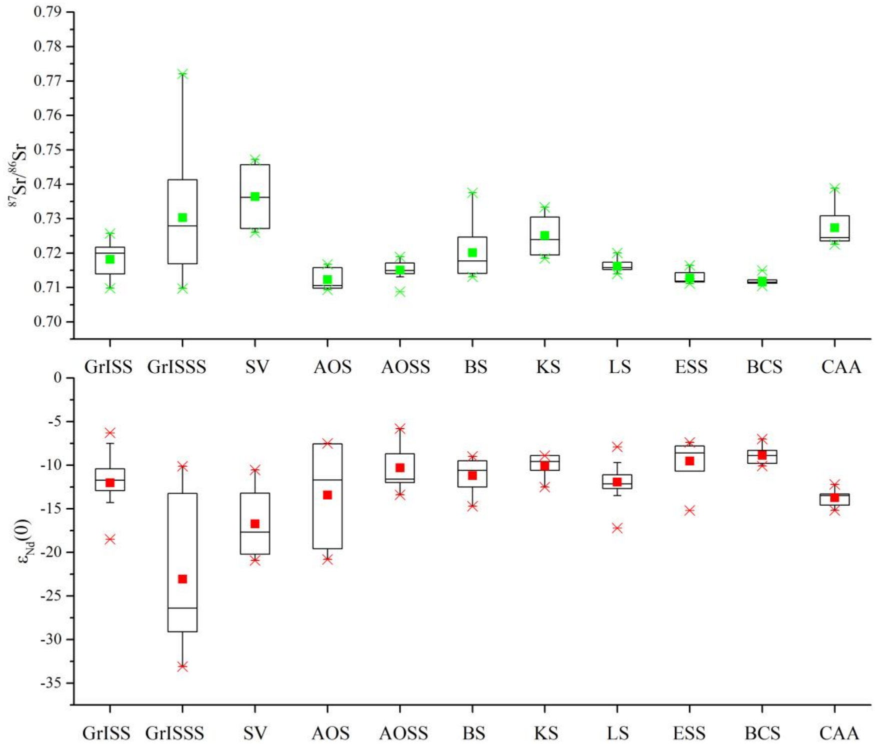

Fig. 6. Box plot for the Sr-Nd isotopic signatures of the Arctic, including the 11 subregion samples of snow, sand, soil, sediment from sea ice and sediment cores.

The Sr-Nd data from Arctic shelf surface sediment were based on the literature (Fig. 6), and the Sr-Nd isotopic compositions in most samples were sieved at < 45 μm for bulk. These data were chosen at water depths < 200 m and the surface or 0-10 cm from the top to better represent the characteristics of coastal terrestrial sources (Maccali et al., 2018). The Sr-Nd data in the BS, KS, LS, ESS, BCS and MCAA surface sediment cores corresponded mainly to drainage basins and their adjacent seas (Maccali et al., 2018). The sample spatial coverage in each region is variable, and Fig.

6 shows the relative homogeneity/heterogeneity for each region as well as isotopic value overlaps. The box plot for these regions of the Arctic are further extended.

3.3. Information on Sr-Nd data from the SH and Antarctic ice sheet

By integrating the literature and adding data with new evidence, the pretreatment method and characteristics of Sr-Nd are discussed in low-latitude SH. Dust provenances of low-elevation areas on the periphery of the Antarctic ice sheet in the modern and paleoenvironment were discussed. This study provides a comprehensive overview of the state of knowledge of dust sources in different sectors of the Antarctic ice sheet and PSAs in the SH under modern and ancient environments.

3.3.1 Sr-Nd characteristics of SH potential dust sources

There are three PSAs in the SH, including Australia, southern South America (hereafter SSA) and Southern Africa (SA)). The Sr and Nd isotopic measurements were taken exclusively on the <5 μm grain size fraction of Australian dust samples. $^{87}Sr/^{86}Sr$ ratios ranging from 0.709 to 0.732 and $\varepsilon_{Nd}(0)$ values in Australian dust samples between -15 and -3, some samples were well-dated samples deposited during glacial periods (Revel-Rolland et al., 2006). Gaiero (2007) identified three main dust sources in SSA with different grain sizes (bulk, 63 μm, 5 μm): the Puna (22–26 °S)/Altiplano (15–22 °S) Plateau, with less radiogenic Nd (-9–-6 for $\varepsilon_{Nd}(0)$); central-western Argentina (27–35 °S), with more radiogenic Nd (-6–-2 for $\varepsilon_{Nd}(0)$); and Patagonia (39–52 °S) with more radiogenic Nd (-1–1 for $\varepsilon_{Nd}(0)$). The isotopic compositions of aeolian dust from Argentina and Chile are confined to the ranges of 0.7045< $^{87}Sr/^{86}Sr$ <0.7130 and -5 <$\varepsilon_{Nd}(0)$ <3. The $^{87}Sr/^{86}Sr$ ratios in sand samples from SA varied between 0.712348 and 0.74716, and the $\varepsilon_{Nd}(0)$ ratios varied between -24.5 and -8.4 (Delmonte et al., 2003; Gili et al., 2021). In addition, the Sr and Nd isotopic compositions in New Zealand sand samples were measured in the <5 μm

https://doi.org/10.5194/essd-2022-91
Preprint. Discussion started: 16 March 2022

Open Access Earth System Science Data Discussions

fraction according to Stoke's Law through humid sedimentation and separated from PSA samples using a syringe; the values ranged from 0.70518 to 0.72324 for $^{87}Sr/^{86}Sr$ and -7.2 to -1.2 for $\varepsilon_{Nd}(0)$ (Delmonte, 2003). The fine fraction (<5 μm) of the Namibia Sand Sea samples of SA was also separated following Stoke's Law by Gili et al. (2021). The Sr-Nd data from PSAs were primarily measured by two references (Delmonte et al., 2003; Gili et al., 2021). The measurement method is almost the same, and these data can very clearly distinguish geographic subgroups for PSAs in SH.

3.3.2 Sr-Nd data on the periphery and interior of the Antarctic ice sheet

Sr-Nd data from Antarctica surface snow layers with different thicknesses (6.5-10 cm) were measured with a three-metre long and one-metre wide snow pit using a stainless steel saw (Bory et al., 2010). Sr-Nd data along the Zhongshan-Dome A transect at 5–6 cm thick were measured using a Teflon shovel and the snow samples were placed in 5 L Whirl-Pak bags (approximately 4–5 bags were collected at each site) (Du et al., 2018). The $\varepsilon_{Nd}(0)$ values of marine sediment (near-core-top samples, 63 μm) from seven sectors of Antarctica are presented in Fig. 7 (Hemming et al., 2007). Sr-Nd isotope data from coastal and low-elevation sites were also collected in ice-free areas near the Filchner–Ronne Ice Shelf, Ross Ice Shelf and Amery Ice Shelf (Fig. 7). The Sr and Nd isotopic compositions of four sand samples from southern King George Island (South Shetland Islands) in West Antarctica, with less radiogenic $^{87}Sr/^{86}Sr$ values ranging from ~0.703907 to ~0.704157 and $\varepsilon_{Nd}(0)$ values ranging from 4.6 to 6.4, are relatively close to the $\varepsilon_{Nd}(0)$ values of marine sediment (near-core-top samples) from the Antarctic Peninsula (ranging from -3 to 1) (Hemming et al., 2007). The $^{87}Sr/^{86}Sr$ ratios ranged from 0.71135 to 0.72377, and the $\varepsilon_{Nd}(0)$ composition ranged from -13.3 to -9.6 from ice-free areas of Inexpressible Island in the Ross Sea, West Antarctica. The measurement method of sand samples

https://doi.org/10.5194/essd-2022-91
Preprint. Discussion started: 16 March 2022

Earth System Science Data
Open Access Discussions

(<71 μm fraction) from southern King George Island and Inexpressible Island is the same as that for the Zhongshan and Progress station sand samples from the Amery Ice Shelf (Du et al., 2018). Based on the Sr-Nd data in our own and the literature (Table 4), four regions were divided in the SH:

Region A: McMurdo, King George Island and SSA (Patagonia), with the highest $\varepsilon_{Nd}(0)$ value of >-5.0;

Region B: Victoria Land, southern Australia, New South Wales, SA and SSA (Puna–Altiplano area), with large variations in $^{87}Sr/^{86}Sr$ values and moderate $\varepsilon_{Nd}(0)$ values, and Taylor Glacier zero-age ice samples are very close to those of samples from Victoria Land and the McMurdo dry valleys;

Region C: northern Australia, Victoria Land sources (including Inexpressible Island) and SA, with high $^{87}Sr/^{86}Sr$ ratios and low $\varepsilon_{Nd}(0)$ values;

Region D: SA, northern Australia and the Amery Ice Shelf, with the lowest $\varepsilon_{Nd}(0)$ values of <-15.

Among these regions, although the data have significant differences, the Sr and Nd compositions of some of the endmembers are similar, and care must be taken when directly comparing these data to precisely explain the observed isotopic compositions in ice core records. For example, there is overlap of the Sr and Nd isotopic compositions of King George Island, SSA (Patagonia) and McMurdo dry valleys. The new Sr and Nd data from Inexpressible Island also overlap with the other endmembers (SA, New South Wale and Prydz Bay). Therefore, dust from low-latitude regions (New South Wale and SA) cannot be excluded from East Antarctica (Du et al., 2018; Gili et al., 2021). Another example is the characteristics of snow layers at the Berkner Island ice sheet in western Antarctica. These data can be partly explained by the surface sediment samples from the Weddell Sea sector, with $\varepsilon_{Nd}(0)$ values ranging

https://doi.org/10.5194/essd-2022-91
Preprint. Discussion started: 16 March 2022

from -10 to -8 (Hemming et al., 2007). Therefore, the dataset from the SH and Antarctic ice sheet demonstrates that multiple mixed sources can be inferred for Antarctic surface snow samples. However, it should be noted that among the data from the entire Antarctica ice sheet, Sr-Nd isotopic components were measured in only 29 snow samples, and there is an urgent need to collect more data in the future.

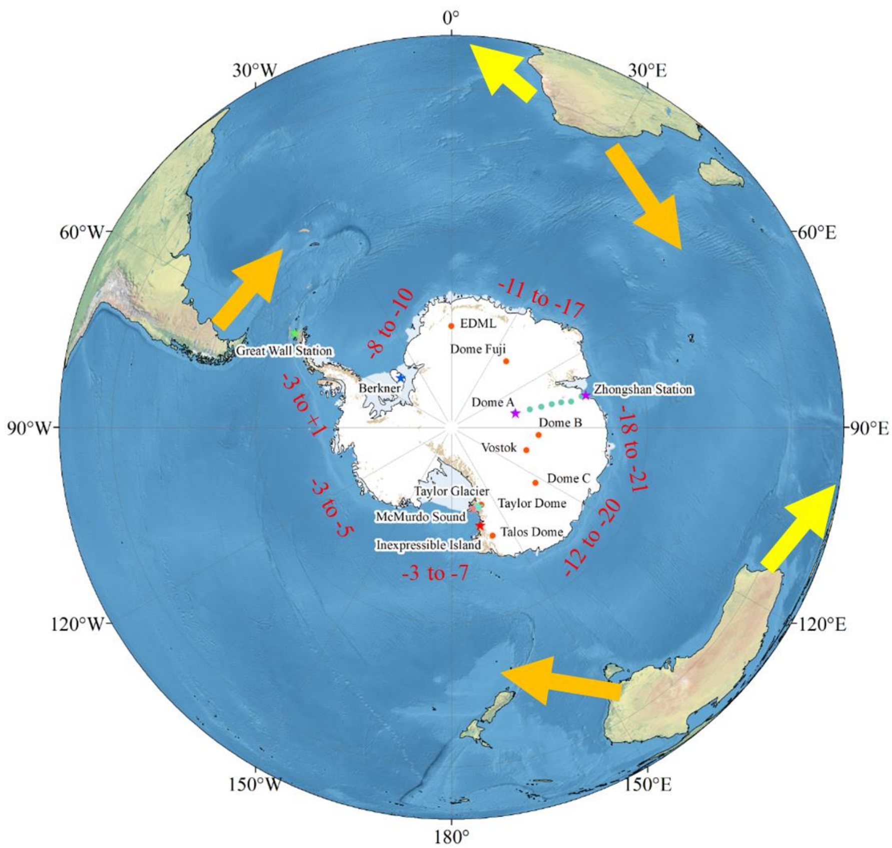

Fig. 7. Surface snow or snowpit samples are represented by purple solid circles, ice core samples represent blue rectangles and samples represent red solid circles. Data sources: Grousset et al., 1992; Basile et al., 1997; Delmonte et al., 2003, 2004, 2008, 2010, 2013 a and b; 2017, 2019; Gaiero, 2007; Revel-Rolland et al. (2006); Aarons et al., 2016; 2017; Du et al., 2018. The sampling sites are noted with red circles (Table

https://doi.org/10.5194/essd-2022-91
Preprint. Discussion started: 16 March 2022

S4). The dust transport paths are marked with yellow arrows. Each sector is characterized by a range of $\varepsilon_{Nd}(0)$ values by S. R. Hemming et al. (2007) (This figure was created with ArcGIS).

3.3.3 Sr and Nd data from Antarctic deep ice cores

Information on Sr-Nd data in Antarctic ice cores during the Holocene and glacial-interglacial times is presented by integrating literature (Table 4). To obtain Sr-Nd data, mineral dust from EPICA-Dome C and Vostok ice core was extracted by filtration using 0.4 μm membranes. Each filter was put into a precleaned Corning tube filled with ~10 mL Milli-Q water, and microparticles were removed from the filter through sonication. The liquid was then evaporated in a clean hood dedicated to chemical preparation of samples for Sr-Nd analyses (Delmonte et al., 2008). To obtain enough dust particles, the different age interval samples were merged. For example, each sample represents approximately 40-160 years for the Vostok ice core, which is a few thousand years to obtain a single large-volume sample (Delmonte et al., 2008). Alternatively, several ice core sections from different depths were integrated to obtain a few large samples for the Sr and Nd isotopic analyses of the Talos Dome ice core (Delmonte et al., 2010b). A relatively high resolution (spanning between ~ 3 and ~ 30 yrs.) was used in the Taylor Dome ice core Sr and Nd were measured using a TIMS equipped with 10^{11} Ohm resistors for $^{87}Sr/^{86}Sr$ ratios and 10^{13} Ohm resistors for $^{143}Nd/^{144}Nd$ ratios (Aarons et al., 2016). Aarons et al. (2017) measured Sr-Nd data in a horizontal ice core of the ablation area from the Taylor Glacier in East Antarctica, which was decontaminated and processed for each ~20 kg ice core sample.

Ice cores are very difficult to obtain and measurement methods limit continuous data. Sr-Nd data in the Antarctica deep ice core mainly focus on the coastal and inland areas of the EAIS. As previously mentioned, the dust source is similar to that of the

https://doi.org/10.5194/essd-2022-91
Preprint. Discussion started: 16 March 2022

modern samples in the Dome C and Vostok ice cores during the Holocene and interglacial periods, which can be explained by an SSA provenance; an additional hypothesis explains the isotopic signature of Holocene dust in central East Antarctica (Delmonte et al., 2008, Delmonte et al., 2019). The Sr-Nd data in the Talos Dome, Taylor Dome and Taylor Glacier ice cores during the Holocene point towards a local dust provenance (Delmonte et al., 2019; Aarons et al., 2016, 2017). Therefore, the Sr and Nd data from East Antarctica ice cores during the Holocene and interglacial periods indicate a well-mixed atmospheric background involving a mixture of two or more sources in the SH (Fig. 8). The newest study demonstrated that SA emerges as the second most important dust source to East Antarctica during interglacial periods (Gili et al., 2021).

However, the glacial stage (stage 4: ~ 60 ka and stage 6: ~ 160 ka) samples in the Vostok ice core span a very narrow range of Sr compositions ($0.708219 < {}^{87}Sr/{}^{86}Sr < 0.708452$) and Nd compositions ($1.1 < \varepsilon_{Nd}(0) < 5.0$), which can also be explained by the new Sr-Nd data in sand samples (<71 μm) from southern King George Island (${}^{87}Sr/{}^{86}Sr$ values ranging from ~0.703907 to ~0.704157 and $\varepsilon_{Nd}(0)$ values ranging from 4.6 to 6.4). The ${}^{87}Sr/{}^{86}Sr$ and $\varepsilon_{Nd}(0)$ isotopic compositions of dust in the Taylor Glacier ice core samples during the last glacial period indicated that dust may originate from SSA and from potential local source areas in the Ross Sea Sector (Delmonte et al., 2010; Aarons et al., 2016; Aarons et al., 2017). Therefore, these data suggest that the glacial-period dust in East Antarctic ice cores also contributes from local contributions (Fig. 8). However, almost no Sr-Nd data were from the West Antarctic deep ice cores, which limits to understand the dust transport in the spatial and temporal distribution of the entire Antarctic ice sheet.

https://doi.org/10.5194/essd-2022-91
Preprint. Discussion started: 16 March 2022

Open Access Earth System Science Data Discussions

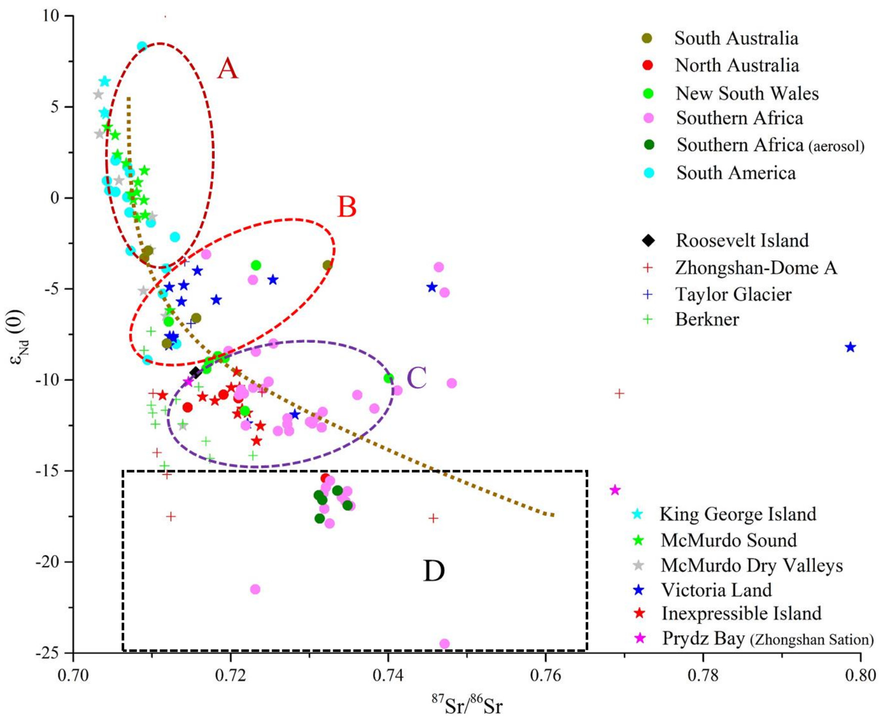

Fig. 8. Sr isotopic composition versus Nd isotopic composition of modern dust deposited in potential dust source areas of Australia (including New South Wales, Revel-Rolland et al., 2006; Grousset et al., 1992), southern Africa (Grousset et al., 1992; Delmonte 2004a; Gili et al., 2021) and South America (Delmonte 2004a) (solid circles with different colours) at the peripheral Antarctic ice sheet of ice-free areas (King George Island and Inexpressible Island, this study; McMurdo Sound, Winton et al., 2014, 2016b; McMurdo Dry Valleys, Gemmiti (2000); Victoria Land, Delmonte et al., 2013; Prydz Bay, Du et al., 2018; stars with different colours), and data obtained on surface snow samples of Antarctic ice sheets with differently coloured crosses (data of Roosevelt Island fromWinton et al., 2016a; data of Zhongshan-Dome A from Du et al., 2018; data of Taylor Glacier from Aarons et al., 2017; data of Berkner from Bory et al., 2010).

4. Data availability

https://doi.org/10.5194/essd-2022-91
Preprint. Discussion started: 16 March 2022

All datasets and the associated metadata table presented in this study are available through a Big Earth Data Platform for Three Poles. The dataset can be downloaded from https://doi.org/10.11888/Cryos.tpdc.272100) (Du et al., 2022). In this repository, the entire datasets are provided in Excel spreadsheet format together with metadata files.

5. Conclusions

The maintenance integrated Sr-Nd dataset was presented from the remote three poles, and these data are not easily collected because of the extremely cold environment. The important conclusion to be drawn from this study is that understanding the dust transport paths of the three poles in a warming environment exposes large source areas of dust. The dataset is complicated and includes snow, sand, soil, loess, deposits, sediment and other types. These integrated data can provide a new perspective into present and paleodust sources from the three poles, more importantly, which clearly emphasizes the following points for potential users of the datasets provided with this paper:

1. This Sr-Nd dataset enables us to map the standardized locations in the remote three poles, while the use of sorting criteria related to the sample location, type or resolution permits us to trace the dust source and sink based on their isotopic signatures.
2. For the third pole, each subregion of Sr-Nd data was provided, and the data will be useful for tracing the local or long-distance transported dust of the source and sink. The integration of these data between sand (soil) and snow samples for six subregions allowed us to clearly understand the Sr-Nd data characteristics in the third pole.
3. There are 11 subregions for the entire Arctic, and Sr-Nd data can provide the user

https://doi.org/10.5194/essd-2022-91
Preprint. Discussion started: 16 March 2022

with sink information on dust in the Arctic environment, which would be useful for tracing dust sources for the Arctic.

4. The new data from Arctic and Antarctica samples emphasized the ice-free regions on the periphery of the ice sheets, which may be important local dust sources. In particular, Sr-Nd data overlap with the low-latitude region of PSAs. However, the paucity of data in Antarctica is serious and future studies should concentrate on this aspect.

Author contributions. CX, ZD, and SA designed the study, ZD, JY, CX and SA wrote the manuscript. ZD, LW, NW, SW, YL collected the samples in field and produced data. ZD, NW, LW, SW, YL, ZW, XM performed analysis. All authors contributed to the final form of the manuscript.

Competing interests. The authors declare that they have no conflict of interest.

This work was supported by the Strategic Priority Research Program of the Chinese Academy of Sciences (XAD19070103), the National Natural Science Foundation of China (Grant Nos. 42071086 and 41971088), the Youth Innovation Promotion Association, CAS (2020419) and the State Key Laboratory of Cryospheric Science (SKLCS-ZZ-2021).

References:

Aarons, S., Aciego, S., Gabrielli, P., Delmonte, B., Koornneef, J., Wegner, A., and Blakowski, M.: The impact of glacier retreat from the Ross Sea on local climate: Characterization of mineral dust in the Taylor Dome ice core, East Antarctica, Earth Planet. Sc. Lett, 444, 34–44, https://doi.org/10.1016/j.epsl.2016.03.035, 2016.

Aarons, S. M., Aciego, S. M., Arendt, C. A., Blakowski, M. A., Steigmeyer, A., Gabrielli, P., SierraHernández, M. R., Beaudon, E., Delmonte, B., Baccolo, G., May, N. W., and Pratt, K. A.: Dust composition changes from Taylor Glacier (East Antarctica) during the last glacial-interglacial transition: A multi-proxy approach, Quat. Sci. Rev, 162, 60-71, https://doi.org/10.1016/j.quascirev.2017.03.011, 2017.

Basile, I., Grousset, F. E., Revel, M., Petit, J. R., and Barkov, N. I.: Patagonian origin of glacial dust deposited in east Antarctica (Vostok and Dome C) during glacial stages 2, 4 and 6. Earth Planet. Sci. Lett, 146(3), 573–589. https://doi.org/10.1016/S0012-821X(96)00255-5, 1997.

Biscaye, P.E., Grousset, F.E., Revel, M., Van der Gaast, S., Zielinski, G.A., Vaars, A., and Kukla, G.: Asian provenance of glacial dust (stage 2) in the Greenland Ice Sheet Project 2 ice core, Summit, Greenland. J. Geophys. Res.-Oceans, 102, 26765-26781. https://doi.org/10.1029/97JC01249, 1997.
Blanchet C L.: A database of marine and terrestrial radiogenic Nd and Sr isotopes for tracing earth-surface processes. Earth Syst. Sci. Data, 11(2):741-759. https://doi.org/10.5194/essd-11-741-2019, 2019.
Bory, J. M., Biscaye, P. E., Svensson, A., and Grousset, F. E.: Seasonal variability in the origin of recent atmospheric mineral dust at NorthGRIP, Greenland. Earth Planet. Sc. Lett, 196(3-4):123-134. https://doi.org/10.1016/S0012-821X(01)00609-4, 2002.
Bory, A.M., Biscaye, P.E., Piotrowski, A.M., Steffensen, J.P.: Regional variability of ice core dust composition and provenance in Greenland. Geochem. Geophy. Geosy, 4. https://doi.org/10.1029/2003GC000627, 2003a.
Bory, A.J.M., Biscaye, P.E., Grousset, F.E.: Two distinct seasonal Asian source regions for mineral dust deposited in Greenland (NorthGRIP). Earth Sci. Rev, 30. https://doi.org/10.1029/2002GL016446, 2003b.
Bory, A., Wolff, E., Mulvaney, R., Jagoutz, E., Wegner, A., Ruth, U., and Elderfield, H.: Multiple sources supply eolian mineral dust to the atlantic sector of coastal antarctica: evidence from recent snow layers at the top of Berkner island ice sheet, Earth Planet. Sci. Lett, 291(1-4), 138-148, https://doi:10.1016/j.epsl.2010.01.006, 2010.
Bory, A.J., Abouchami, W., Galer, S.J., Svensson, A., Christensen, J.N., and Biscaye, P.E.: A Chinese imprint in insoluble pollutants recently deposited in central Greenland as indicated by lead isotopes. Environment Science & Technology, 48, 1451-1457, https://doi.org/10.1021/es4035655, 2014.
Chen, J., Li, G., Yang, J., Rao, W., Lu, H., Balsam, W., Sun, Y., and Ji, J.: Nd and Sr isotopic characteristics of Chinese deserts: implications for the provenances of Asian dust. Geochimica Et Cosmochimica Acta, 71, 3904-3914, https://doi.org/10.1016/j.gca.2007.04.033, 2007.
Delmonte, B., Quaternary variations and origin of continental dust in East Antarctica, PhD Thesis, Università degli Studi di Siena / Université Joseph Fourier - Grenoble 1, 2003.
Delmonte, B., Basile-Doelsch, I., Petit, J. R., Maggi, V., Revel-Rolland, M., Michard, A., Jagoutzg. E., and Grousset, F.: Comparing the Epica and Vostok dust records during the last 220,000 years: stratigraphical correlation and provenance in glacial periods. Earth Sci. Rev, 66(1-2), 63-87, https://doi.org/10.1016/j.earscirev.2003.10.004, 2004a.
Delmonte, B., Petit, J.R., Andersen, K.K., Basile-Doelsch, I., Maggi, V., Lipenkov, V.: Dust size evidence for opposite regional atmospheric circulation changes over East Antarctica during the last climatic transition. Clim. Dyn 23, 427–438. DOI 410.1007/s00382-00004-00450-00389, 2004b.
Delmonte, B., Andersson, P.S., Hansson, M., Schoberg, H., Petit, J.R., Basile-Doelsch, I., and Maggi, V.: Aeolian dust in East Antarctica (EPICA-Dome C and Vostok): provenance during glacial ages over the last 800 kyr. Geophys. Res. Lett, 35 (7), L07703, https://doi:10.1029/02008GL033382, 2008.
Delmonte, B., Andersson, P.S., Schoberg, H., Hansson, M., Petit, J.R., Delmas, R., Gaiero, D.M., Maggi, V., and Frezzotti, M.: Geographic provenance of Aeolian dust in East Antarctica during Pleistocene glaciations: preliminary results from Talos Dome and comparison with East Antarctic and new Andean ice core data. Quat. Sci. Rev, 29, 256–264,

https://doi.org/10.5194/essd-2022-91
Preprint. Discussion started: 16 March 2022

https://doi.org/10.1016/j.quascirev.2009.05.010, 2010a.

Delmonte, B., Baroni, C., Andersson, P.S., Schöberg, H., Hansson, M., Aciego, S., Petit, J.-R., Albani, S., Mazzola, C., Maggi, V., and Frezzotti, M.: Aeolian dust in the Talos Dome ice core (East Antarctica, Pacific/Ross Sea sector): Victoria Land versus remote sources over the last two climate cycles. J. Quat. Sci, 25 (8), 1327–1337, https://doi.org/10.1002/jqs.1418, 2010b.

Delmonte, B., Baroni, C., Andersson, P. S., Narcisi, B., Salvatore, M. C., Petit, J. R., Scarchilli, C., Frezzotti, M., Albani, S., and Maggi, V.: Modern and Holocene aeolian dust variability from Talos Dome (Northern Victoria Land) to the interior of the Antarctic ice sheet, Quaternary Sci. Rev, 64, 76–89, doi:10.1016/j.quascirev.2012.11.033, 2013.

Delmonte, B., Paleari, C. I., Andò, S., Garzanti, E., Andersson, P. S., Petit, J. R., Crosta, X., Narcisi, B., Baroni, C., Salvatore, M., Baccolo, G., and Maggi.: Causes of dust size variability in central East Antarctica (Dome B): Atmospheric transport from expanded South American sources during Marine Isotope Stage 2. Quaternary Sci. Rev, 168, 55– 68, https://doi.org/10.1016/j.quascirev.2017.05.009, 2017.

Delmonte, B., Winton, H., Baroni, M., Baccolo, G., Hansson, M., Andersson, P., Baroni, C., Salvatore, M., Lanci, L., and Maggi, V.: Holocene dust in East Antarctica: provenance and variability in time and space. Holocene, 30 (4), 546-558, https://doi.org/10.1177/0959683619875188, 2019.

Dong, Z., Kang, S., Qin, D., Wang, X., Ren, J., Li, X., Yang, J., and Qin, X.: Provenance of cryoconite deposited on the glaciers of the Tibetan Plateau: new insights from Nd-Sr isotopic composition and size distribution. J. Geophys. Res.: Atmosphere, 121 (12), 7371-7382, http://doi.org/10.1002/2016JD024944, 2016.

Dong, Z., Shao, Y., Qin, D., Kang, S., Wei, W., Wang, X., and Wang, S.: Hf-Nd-Sr isotopic composition as fingerprint for long-range transported eolian dust deposition in glacier snowpack of eastern Tibetan Plateau. J. Geophys. Res, 123, 7013–7023, https://doi.org/10.1029/2018JD028581, 2018.

Du, Z., Xiao, C., Liu, Y., Wu, G.: Geochemical characteristics of insoluble dust as a tracer in an ice core from Miaoergou Glacier, east Tien Shan. Glob. Planet. Chang, 127, 12-21. http://doi.org/10.1016/j.gloplacha.2015.01.011, 2015.

Du, Z., Xiao, C., Ding, M., and Li, C.: Identification of multiple natural and anthropogenic sources of dust in snow from Zhongshan Station to Dome A, East Antarctica. J. Glaciol, 64: 855–865, https://doi.org/10.1017/jog.2018.72, 2018.

Du, Z., Xiao, C., Wang, Y., Liu, S., and Li, S.: Dust provenance in Pan-third pole modern glacierized regions: What is the regional source?. Environmental Pollution, 250(JUL.): 762-772, https://doi.org/10.1016/j.envpol.2019.04.068, 2019a.

Du, Z., Xiao, C., Dou, T., Li, S., An, H., Liu, S., and Liu K.: Comparison of Sr–Nd–Pb isotopes in insoluble dust between northwestern China and high-latitude regions in the Northern Hemisphere. Atmospheric Environment, 214:116837, https://doi.org/10.1016/j.atmosenv.2019.116837, 2019b.

Gaiero, D.M.: Dust provenance in Antarctic ice during glacial periods: from where in southern South America? Geophys. Res. Lett. 34 (17), https://doi.org/10.1029/2007GL030520, 2007.

Gaiero, D.M., Brunet, F., Probst, J.L., Depetris, P.J.: A uniform isotopic and chemical signature of dust exported from Patagonia: rock sources and occurrence in southern environments. Chem. Geol. 238 (1), 107-120, https://doi.org/10.1016/j.chemgeo.2006.11.003, 2007.

Gili, S., Vanderstraeten, A., Chaput, A., King, J., Gaiero, D., Delmonte, B., Vallelonga, P., Formenti, P., Di Biagio, C., Cazanau, M. and Pangui, E.: Southern Africa: The Missing Piece To The Dust Provenance Puzzle of East Antarctica? Communications Earth & Environment, 2021.

https://doi.org/10.5194/essd-2022-91
Preprint. Discussion started: 16 March 2022

Grousset, F. E., Biscaye, P. E., Revel, M.., Petit, J., Pye, K., Joussaume, S., and Jouzel, J.: Antarctic (Dome C) ice-core dust at 18 k.y. B. P.: isotopic constraints on origins, Earth Planet. Sci. Lett, 111, 175–182, https://doi.org/10.1016/0012-821X(92)90177-W, 1992.

Grousset, F. E., Parra, M., Bory, A., Martinez, P., Bertrand, P., Shimmield, G and Ellam, R. M.: Saharan wind regimes traced by the Sr–Nd isotopic composition of subtropical Atlantic sediments: last glacial maximum vs today, Quaternary Sci. Rev, 17, 395–409, https://doi.org/10.1016/S0277-3791(97)00048-6, 1998.

Han, C., Hur, S. D., Han, Y., Lee, K., Hong, S., Erhardt, T., Fischer, H., Svensson, A., Steffensen, JP., and Vallelonga, P.: High-resolution isotopic evidence for a potential Saharan provenance of Greenland glacial dust. Sci Rep, 8, 15582, https://doi.org/10.1038/s41598-018-33859-0, 2018.

Hemming, S.R., van de Flierdt, T., Goldstein, S.L., Franzese, A.M., Roy, M., Gastineau, G., Landrot, G.: Strontium isotope tracing of terrigenous sediment dispersal in the Antarctic Circumpolar Current: implications for constraining frontal positions. Geochem. Geophys. Geosyst, 8 (6), Q06N13, https://doi:10.1029/2006GC001441, 2007.

Jacobsen, S.B., Wasserburg, G.J. (1980) Sm-Nd evolution of chondrites. Earth Planet. Sci. Lett. 50, 139-155.

Lambert, F., Kug, J. S., Park, R. J., Mahowald, N., Winckler, G., Abe-Ouchi, A., and Lee, J. H.: The role of mineral-dust aerosols in polar temperature amplification, Nat. Clim. Change, 3, 487–491, https://doi.org/10.1038/nclimate1785, 2013.

Livingstone I and Warren A (1996) Aeolian Geomorphology. Singapore: Addison Wesley Longman Ltd.

Lupker, M., Aciego, S.M., Bourdon,B., Schwander,J., and Stocker, T.F.: Isotopictracing(Sr, Nd, U and Hf) of continental and marine aerosols in an 18th century section of the Dye-3 ice core (Greenland). Earth Planet. Sci. Lett, 295. http://dx.doi.org/10.1016/j.epsl.2010.04.010, 2010.

Maccali, J., Hillaire-Marcel, C., Not, C.: Radiogenic isotope (Nd, Pb, Sr) signatures of surface and sea ice-transported sediments from the Arctic Ocean under the present interglacial conditions. Polar Research, 37(1):1442982, 2018. https://doi.org/10.1080/17518369.2018.1442982.

Nagatsuka, N., Takeuchi, N., Uetake, J., Shimada, R., Onuma, Y., Tanaka, S., and Nakano, T.: Variations in Sr and Nd isotopic ratios of mineral particles in cryoconite in Western Greenland. Frontiers in Earth Science 4, 93, https://doi.org/10.3389/feart.2016.00093, 2016.

Revel-Rolland M, De Deckker, P., Delmonte, B., Hesse, P.P., Magee, J.W., Basile-Doelsch, Grousset, F., and Bosch, D.: Eastern Australia: A possible source of dust in East Antarctica interglacial ice. Earth Planet. Sc. Lett, 249(1–2): 1–13, https://doi.org/10.1016/j.epsl.2006.06.028, 2006.

Rex, D. C. and Gledhill, A. R.: Isotopic studies in the East Greenland Caledonides (72 °-74 °N)-Precambrian and Caledonian ages. Rapp. Grønlands Geologiske Undersøgelse 104, 47–72 (1981).

Ruan, X., Yang, Y., Galy, A., Fang, X., Zhang, W.: Evidence for early ($\geqslant$12.7 Ma) eolian dust impact on river chemistry in the northeastern tibetan plateau. Earth and Planetary Science Letters, 515, 79-89, https://doi.org/10.1016/j.epsl.2019.03.022, 2019.

Simonsen, M. F., Baccolo, G., Blunier, T., Borunda, A., Delmonte, B., Frei, R., Goldstein, S., Grinsted, A., Kjær, A.A., Sowers, T., Svensson, A., Vinther, B., Vladimirova, D., Winckler, G., Winstrup, M., and Vallelonga, P.: East Greenland ice core dust record reveals timing of Greenland ice sheet advance and retreat. Nature Communications, 10(1):1-8, https://doi.org/10.1038/s41467-019-12546-2, 2019.

https://doi.org/10.5194/essd-2022-91
Preprint. Discussion started: 16 March 2022

Struve, T., Pahnke, K., Lamy, F., Wengler, M., Böning, P., Winckler, G.: A circumpolar dust conveyor in the glacial Southern Ocean. Nature Communications, 11(1), 1–11. https://doi.org/10.1038/s41467-020-18858-y, 2020.

Svensson, A., Biscaye, P.E., Grousset, F.E.: Characterization of late glacial continental dust in the Greenland Ice Core Project ice core. J. Geophys. Res.: Atmosphere, 105, 4637-4656, https://doi.org/10.1029/1999JD901093, 2000.

Újvári, G., Stevens, T., Svensson, A., Klötzli, U.S., Manning, C., Németh, T., Kovács, J., Sweeney, M.R., Gocke, M., Wiesenberg, G.L.B., Markovic, S.B., Zech, M.: Two possible source regions for central Greenland last glacial dust. Geophys. Res. Lett. 42, 10,399–310, 408, https://doi.org/10.1002/2015GL066153, 2015.

Wei, T., Dong, Z., Kang, S., Qin, X., Guo, Z.: Geochemical evidence for sources of surface dust deposited on the Laohugou glacier, Qilian Mountains. Appl. Geochem. 79, 1-8. http://doi.org/10.1016/j.apgeochem.2017.01.024, 2017.

Wei, T., Dong, Z., Kang, S., Rostami, M., Ulbrich, S., and Shao, Y.: Hf-Nd-Sr isotopic fingerprinting for aeolian dust deposited on glaciers in the northeastern Tibetan Plateau region. Glob. Planet. Chang, 177, 69–80, https://doi.org/10.1016/j.gloplacha.2019.03.015, 2019

Wei, T., Brahney, J., Dong, Z., Kang, S., Zong, C., Guo, J., Yang, Lin., Qin, X.: Hf-Nd-Sr Isotopic Composition of the Tibetan Plateau Dust as a Fingerprint for Regional to Hemispherical Transport. Environmental Science & Technology, 55(14). https://doi.org/10.1021/acs.est.0c04929, 2021.

Wu, G., Zhang, C., Zhang, X., Tian, L., Yao, T.: Sr and Nd isotopic composition of dust in Dunde ice core, Northern China: implications for source tracing and use as an analogue of long-range transported Asian dust. Earth Planet. Sci. Lett, 299 (3), 409-416. http://doi.org/10.1016/j.epsl.2010.09.021, 2010.

Xu, J., Yu, G., Kang, S., Hou, S., Zhang, Q., Ren, J., Qin, D.: Sr-Nd isotope evidence for modern aeolian dust sources in mountain glaciers of western China. J. Glaciol, 58 (211), 859-865. http://doi.org/10.3189/2012JoG12J006, 2012.

Winton, V. H. L., Edwards, R., Delmonte, B., Ellis, A., Andersson, P. S., Bowie, A., Bertler, N. A. N., Neff, P., and Tuohy, A.: Multiple sources of soluble atmospheric iron to Antarctic waters, Global Biogeochem. Cy., 30, 421–437, https://doi.org/10.1002/2015GB005265, 2016a.

Winton, V., Dunbar, G. B., Atkins, C. B., Bertler, N., Delmonte, B., Andersson, P. S., Bowie, A., and Edwards, R.: The origin of lithogenic sediment in the south-western ross sea and implications for iron fertilization. Antarctic Science, 28(4), 250-260, https://doi.org/10.1017/S095410201600002X, 2016b.

Zhao, W., Balsam, W., Williams, E., Long, X., and Ji, J.: Sr–Nd–Hf isotopic fingerprinting of transatlantic dust derived from North Africa. Earth Planet. Sc. Lett, 486, 23-31, https://doi.org/10.1016/j.epsl.2018.01.004, 2018.

https://doi.org/10.5194/essd-2022-91
Preprint. Discussion started: 16 March 2022

Open Access Earth System Science Data Discussions

Table 1. Data distribution locations and sample types for $^{87}Sr/^{86}Sr$ and $\varepsilon_{Nd}(0)$ from 42 references.

Location	Sample type	Data points	$^{87}Sr/^{86}Sr$	$\varepsilon_{Nd}(0)$	References
Third Pole		274			
Altai Mountains	Snow/Sand	12	Yes	Yes	Chen et al., 2007; Xu et al., 2012; Du etal., 2019a
Tienshan and Kunnun Mountains (including	Snow/Ice/sand	45	Yes	Yes	Chen et al., 2007; Nagatsuka et al., 2010; Xu et al., 2012; Du et al., 2015; Du et al., 2019a; Wei et al.,
Central Tibet Plateau	Snow/Sand	39	Yes	Yes	Xu et al., 2012; Du et al., 2019a; Wei et al., 2019
Himalaya Mountains	Snow/Sand	34	Yes	Yes	Xu et al., 2012; Du et al., 2019a; Wei et al., 2019
Qiliuan Mountains	Snow/Ice/Sand	50	Yes	Yes	Wu et al., 2010; Xu et al., 2012; Dong et al., 2018; Du
Heduan Mountains	Snow/Sand	24	Yes	Yes	Xu et al., 2012; Dong et al., 2018; Wei et al., 2021
Other deserts and loess in China	Sand/Loess	70	Yes	Yes	Chen et al., 2007; Du et al., 2019a
Arctic		205			
Greenland	Snow/Ice/Cryoconite/Sediment	186	Yes	Yes	Biscaye et al., 1997; Svensson et al., 2000; Bory et al., 2002; Bory et al., 2003a; Lupker et al., 2010; Nagatsuka et al., 2016; Han et al., 2018; Simonsen et al., 2019
Svalbard	Snow/Sand/Loess	7	Yes	Yes	Du et al., 2019b
Arctic Ocean	Snow/Sediment	104	Yes	Yes	Maccali et al., 2018; Du et al., 2019b; this study
Alaska	Snow/Sand/Loess	5	Yes	Yes	Du et al., 2019b
Antarctica		354			
East Antarctica	Snow/Sand	215	Yes	Yes	Paolo et al., 1982; Grousset et al., 1992; Basile et al. 1997; Gemmiti, 2000; Delmonte, 2003; Delmonte et al., 2004 a, b; Delmonte et al., 2007; Delmonte et al., 2008; Delmonte et al., 2010a; Delmonte et al., 2013; Aarons et al., 2016; Winton et al., 2016 a, b; Delmonte et al., 2017; Aarons et al., 2017; Du et al., 2018
West Antarctica	Snow/Ice/Sand/Aeolian deposits/Rock	27	Yes	Yes	Bory et al., 2010; Delmonte et al., 2010b; Winton et al., 2016a; this study
Southern American	Loess/Soil/Sediment/Aeolian	57	Yes	Yes	Grousset, et al., 1992; Basile et al., 1997; Delmonte,
Southern Africa	Aeolian dust/Loess	24	Yes	Yes	Grousset, et al., 1992; Delmonte, 2003; Gili.,et al., 2021
Australia	Sand/Loess/Sediment	15	Yes	Yes	Grousset, et al., 1992; Revel-Rolland et al., 2007

https://doi.org/10.5194/essd-2022-91
Preprint. Discussion started: 16 March 2022

Table 2. Snow, sand and soil samples were located in the third pole glaciers and PSAs of dust generation. Headers from left to right: Label: the number of glaciers; Subregions; Glacier name; Site name: name of the sampling site where the samples were taken; Longitude and Latitude; sampling location; Sample type: Snow, sand or soil; Elevation: m a.s.l; Isotopic ratios of Sr and $\varepsilon_{Nd}(0)$; Ref.: reference publications. The different colours represent different subregions.

Label	Sub-regions	Glacier name	Site name	Latitude (°N)	Longitude (°E)	Mountains	Sample type	Elevation (m a.s.l)	$^{86}Sr/^{87}Sr$	$\varepsilon_{Nd}(0)$	Ref
1	Region I	Musidao	MSD	47°06′N	85°33′E	Altai mountains	Snow	3605	0.713185–0.713571	-6.55–-4.80	Xu et al., 2012
2		Muztagata	MS	38°17′N	75°06′E	East Pamirs	Snow	6365	0.717187–0.717415	-10.3–-8.4	Xu et al., 2012
3	Region II	Tienshan No. 1	TS/UM	43°07′N	86°49′E	Tien Shan	Snow/Surface dust	4063	0.719404–0.721728	-10.9–-6.9	Nagatsuka et al., 2010; Xu et al., 2012
4		Miaoergou	MG	43°03′19″N	94°19′21″E	Tiean Shan	Ice/Snowpack/Cryoconite	3100–4512	0.710284–0.720825	-11.6–-7.3	Du et al., 2015; Wei et al., 2019
5		Yuzhufeng Glacier	YG-1	35°39′37″ N	94°14′28″E	Kulun Mountains	Snow	4300–4720	0.714821–0.716757	-16.6–-11.8	Wei et al., 2019
6		Zangsegangri	ZSGR	34°16′N	85°51′E	Qiangtang plateau	Snow	6226	0.717352–0.718328	-12.9–-9.2	Xu et al., 2012
7	Region III	Guoqu	GL	33°35′N	91°12′E	Tanggula mountains	Snow	5765	0.717546–0.721786	-10.2–-9.5	Xu et al., 2012
8		Dongkemadi	DKMD	33°06′N	92°06′E	Tanggula mountains	Snow	5700	0.713192	–10.51	Xu et al., 2012
9		Zadang	ZD	30°28′N	90°39′E	Nyainqentanglha	Snow	5758	0.718285–0.721305	-12.9–-11.1	Xu et al., 2012
10		Jiemayangzong	JMYZ	30°13′N	82°10′E	Himalaya	Snow	5558	0.72671–0.740694	-14.3–-10.5	Xu et al., 2012
11	Region IV	Yala	Yala	28°14′E	85°37′N	Himalaya	Snow	5190	0.740112	-15.68	Xu et al., 2012
12		East Rongbuk	QM	28°06′N	86°58′E	Himalaya	Snow	6525	0.728057–0.757407	-28.1–-14.7	Xu et al., 2012
13		Laohugou Glacier No.12	LHG	39°26′N	96°32′E	Qilian Mountains	Snow	4288–5026	0.720448–0.723303	-15.7–-9.5	Xu et al., 2012; Wei et al., 2019
14		Dunde ice cap	DD	38°06′N	96°24′E	Qilian Mountains	Ice	5325	0.715220–0.721874	-11.1–-9.9	Wu et al., 2010
15		Qiyi Glacier 1	QG	39°14′13″N	97°45′20″E	Qilian mountains	Snow	4500–4750	0.712349–0.722751	-13.7–-8.6	Dong et al., 2018
16	Region V	Shiyi Glacier	SD	38°12′45″N	99°52′40″E	Qilian mountains	Snow	3928–4152	0.721032–0.721711	-14.0–-13.8	Wei et al., 2019
17		Dabanshan	DS	37°21′43″N	101°24′12″ E	Qilian mountains	Snow	3593–3625	0.723105–0.725015	-12.1–-12.0	Wei et al., 2019
18		Lenglongling Glacier	LG	37°31′N	101°54′E	Qilian mountains	Snow	3558–3992	0.719084–0.728414	-10.9–-7.0	Dong et al., 2018
19		Dagu Glacier	DG	32°07′ N	102°26′ E	Hengduan mountains	snow	3520–3701	0.719216–0.721102	-16.9–-12.3	Dong et al., 2018
20		Hailuogou Glacier	HG	29°20′ N	101°34′ E	Hengduan mountains	snow	3010–3850	0.722805–0.728326	-17.1–-12.0	Dong et al., 2018
21	Region VI	Demula Glacier	DML	29°22′ N	97°00′ E	Hengduan mountains	Snow	5404	0.729095–0.735863	-17.1–-14.2	Xu et al., 2012
22		Baishui Glacier No.1	YL	27°06′ N	100°12′ E	Hengduan mountains	Snow	4338–4747	0.717145–0.719881	-13.8–-11.4	Xu et al., 2012; Dong et al., 2018

https://doi.org/10.5194/essd-2022-91
Preprint. Discussion started: 16 March 2022

Table 3. Snow, cryoconite, sand, soil and sediment samples located in the Arctic. Headers from left to right: Label; Subregions; name of the sampling site where the samples were taken; Sample type: Snow, Cryoconite, sand and soil; Elevation: m a.s.l; Ref.: reference publications.

Label	Subregion	Location	Sample type	Elevation (m a.s.l)	Time interval	Size fraction	Ref
1	GrISS	East Greenland	snowpit	2702	2017/2018	>0.2 μm	This study
1	GrISS	North Greenland	snowpit	2959	early-1995	<45 or 38 μm	Bory et al., 2002
2	GrISSS	Central East Greenland	Rock, Powder, Sediment	NO	No	bulk	Simonsen et al., 2019
2	GrISSS	West Greenland	Cryoconite, Moraine, Englacial dust, Sand	247	No	bulk	Nagatsuka et al., 2016; This study
3	SV	Arctic Ocean	Sediment	0	No	<100 μm	Tütken et al., 2002; Maccali et al., 2018
3	SV	Ny-Ålesund	Snow, Sand, Soil	0-500	2016	Bulk	Du et al., 2019b
4	AOS	Arctic Ocean	Snow	0	2016	Bulk	Du et al., 2019b; This study
5	AOSS	Arctic Ocean	Sea-ice sediment	0	No	bulk	Tütken et al., 2002; Maccali et al., 2018
6	BS	Arctic Ocean	Sediment	0	No	<100 μm	Maccali et al., 2018
7	KS	Arctic Ocean	Sediment	0	No	<100 μm	Tütken et al., 2002; Maccali et al., 2018
8	LS	Arctic Ocean	Sediment	0	No	<100 μm; Bulk	Eisenhauer et al., 1999; Maccali et al., 2018
9	ESS	Arctic Ocean	Sediment	0	No	<100 μm	Maccali et al., 2018
10	BCS	Arctic Ocean	Sediment	0	No	<100 μm; Detrital	Asahara et al., 2012; Maccali et al., 2018
11	CAA	Arctic Ocean	Sediment	0	No	<100 μm	Maccali et al., 2018

https://doi.org/10.5194/essd-2022-91
Preprint. Discussion started: 16 March 2022

Table 4. Samples information in the SH and Antarctica. Headers from left to right name of the sampling site where the samples were taken; sample numbers; time interval (age); Sample type; Size fraction; Ref.: reference publications.

Site name	Numbers	Time interval (age)	Sample type	Size fraction	Ref
Zhongshan Station-Dome A, East Antarctica	11	2016/2017	Snow	>0.2 µm	Du et al., 2018
Roosevelt Island, West Antarctica	2	2011/2012	Snow	>0.2 µm	Winton et al., 2016a
Surface snow (top ~3 cm), West Antarctica	14	2002/2003	Snow	>0.4 µm	Bory et al., 2010
ITASE, East Antarctica	3	1420–1800 A.D.	Ice	Bulk	Delmonte et al., 2013
Talos Dome, Dome C, Vostok, East Antarctica	6	Holocene	Ice	>0.4 µm	Basile (1997); Delmonte et al., 2010a
Komosmolskaia ice core, East Antarctica	2	Deglaciation	Ice	Bulk	Delmonte et al., 2004b
Talos Dome, Dome B, Dome C, Old Dome C, Vostok, East Antarctica	56	MIS 2, 3, 4, 5, 5.5, 6, 8, 10 and older	Ice	Bulk	Basile et al., 199; Grousset et al., 1992; Delmonte, 2003; Delmonte et al., 2004a; Delmonte et al., 2004b; Delmonte et al., 2008; Delmonte et al., 2010a; Delmonte et al., 2010b; Delmonte et al., 2017
Taylor Glacier, East Antarctica	39	0-45711	Ice	>0.2 µm	Aarons et al., 2017
Taylor Dome, East Antarctica	34	1100-31400	Ice	>0.2 µm and <30 µm	Aarons et al., 2016
Bolivia, Illimani, Southern America	7	1950-1930 A.D.	Ice	<8 µm	Delmonte et al., 2010b
Zhongshan and Progress stations, East Antarctica	2	n.d.	Sand	<71 µm	Du et al., 2018
Inexpressible Island, East Antarctica	11	n.d.	Sand	<71 µm	This study
King George Island, West Antarctica	4	n.d.	Sand	<71 µm	This study
McMurdo Sound, East Antarctica	11	n.d.	Sediment trap	Bulk	Winton et al., 2016b
Ross sea, East Antarctica	2	n.d.	Sediment trap	Bulk	Winton et al., 2016b
Enderby Land, East Antarctica	5	n.d.	Rocks	Bulk	Paolo et al., 1982
Mimy (continental shelf sediments), East Antarctica	1	n.d.	Sediment	Bulk	Basile et al., 1997
Terre Adelie (continental shelf sediments), East Antarctica	3	n.d.	Sediment	Bulk, <5 µm	Grousset, et al., 1992
Bunger Hills (moraines), East Antarctica	2	n.d.	Moraines	Bulk	Basile et al., 1997
Dry valleys, East Antarctica	1	n.d.	Sand	<30 µm	Basile et al., 1997

https://doi.org/10.5194/essd-2022-91
Preprint. Discussion started: 16 March 2022

Victoria Land	14	n.d.	Regolith (granite)	<5 µm	Delmonte et al., 2013
McMurdo Dry Valleys and Northern Victoria Land, East Antarctica	11	n.d.	Aeolian deposits	< 5 µm	Gemmiti, 2000, Delmonte, 2003
South America*	57	n.d.	Loess, Soil, Sediment, Eolian dust, Volcanic materials, Aeolian deposits	Bulk, <5 µm, < 10 µm, < 63 µm	Grousset, et al., 1992, Basile et al., 1997, Delmonte, 2003, Gaiero et al., 2007
Australia*	24	n.d.	Suspended dust, Loess, Sand dune, Lacustrine sediment, Sand dune, Loess-like deposit, Marine sediment	< 5 µm	Grousset, et al., 1992, Revel-Rolland et al., 2007
Africa	53	n.d.	Dust, Loess, Aerosol, Sediment; Aeolian deposits	<5 µm, Fine, Bulk	Grousset, et al., 1992, Delmonte, 2003, Gili et al., 2021
New Zealand	16	n.d.	Loesses, Aeolian deposits	Bulk or < 5 µm	Basile et al., 1997;Gemmiti, 2000; Delmonte, 2003

* means few samples have the dating ages.